DOI: 10.15201/hungeobull.73.4.1 Hungarian Geographical Bulletin **73** 2024 (4) 337–353.

Spatial extension of soil water regime variables derived from soil moisture values using geomorphological variables in Hungary

Tamás DEÁK[1], András DOBAI[1], Zoltán Károly KOVÁCS[1], Ferenc MOLNÁR[1] and Endre DOBOS[1]

Abstract

Accurate measurement and spatial extension of soil properties are essential in geoinformatics and precision agriculture for effective resource management, particularly irrigation planning. This study addresses the challenge of extending soil moisture data and related soil water regime variables in heterogeneous agricultural landscapes by integrating geomorphological variables (GVs) derived from high-resolution digital elevation models (DEM). In digital soil mapping, machine learning and geostatistical models often struggle with validation due to data scarcity and variability across space through many geographical regions that come from the point readings of soil properties. A different approach was developed in the form of a new methodology combining two hourly Sentek soil moisture measurements from the topsoil with DEM-derived GVs to model and extend soil water regime variables. The research was conducted on an agricultural field in a hilly area with diverse geomorphological variability. The model's performance was validated using cross-validation techniques. The monitoring and spatial extension results indicate that GVs enhance the spatial prediction of soil moisture, capturing periodic fluctuations in the upper soil layer more effectively by using in-situ, time series soil moisture sensor readings rather than traditional, on field, one time reading approaches. We observed that certain GVs, such as the slope, both type of curvatures and the convergence, were strong predictors of soil moisture variation, enabling the model to produce more accurate irrigation recommendations for agricultural areas with similar geomorphological areas. One of the soil water regime variables was validated during the preliminary validation with mixed results. The main issue was coming from the field use and spatial scarcity of the measurements. Our approach not only provides a different method for spatially extending the current soil water regime data but also offers a framework for improving irrigation decision-making with the help of other value rates and limit related soil regime variables derived from the time series readings from the soil moisture sensors. With its variables, the model allows for forecasts of soil moisture changes, which can inform better irrigation scheduling and water resource management, all based on data from the soil monitoring sensor system.

Keywords: soil moisture, water characteristics, soil water regime variables, geomorphology, GIS, machine learning, digital elevation model (DEM), precision agriculture

Received August 2024, accepted November 2024.

Introduction

There is a significant demand for soil parameters that describe measured and derived soil properties, both from the agricultural sector and for climate-related research and decision support systems (Van de Broek, M. *et al.* 2019).

[1] Institute of Geography and Geoinformatics, Faculty of Earth- and Environmental Science and Engineering, University of Miskolc. Egyetemváros, HU-3515 Miskolc, Hungary. E-mails – ORCIDs: tamas.deak@uni-miskolc.hu – 0009-0001-1360-4159, andras.dobai@uni-miskolc.hu – 0000-0002-5268-0728, karoly.kovacs@uni-miskolc.hu ⁻ 0000-0002-4872-1136, molnar.ferenc@uni-miskolc.hu – 0009-0006-0470-0129, endre.dobos@uni-miskolc.hu – 0000-0002-9798-6376

In Hungary, while large-scale water resource maps are available for water management, hazards, and related uses, these resources operate only at a general scale (Laborczi, A. *et al.* 2020). This limits their utility in high-precision applications, especially when analyzing the impact of various small-scale landforms – micro-basins, shallow water bodies, or small-scale relief units – on irrigation needs and soil moisture retention. Precision agriculture, which addresses these challenges on a finer scale, has shown considerable promise in optimizing agricultural water management, yet substantial gaps remain in data granularity and methodology (Liang, Z. *et al.* 2020; Garcia, L.D. *et al*. 2023).

In general, traditional machine learning validations – such as dividing existing measured values into training and testing datasets – are difficult to implement due to the lack of localised soil measurements across different study areas. The scarcity and variability of numerical data complicate model validation and call for the development of customized validation methods. These methods should enable a robust assessment of the error magnitude between actual and estimated data. Furthermore, because spatial variables derived from terrain models are highly correlated with soil moisture properties, they hold strong potential for informing soil-related variables, especially those concerning soil water regimes (Dobos, E. *et al.* 2000; Dobos, E. and Daroussin, J. 2005; Olaya, V. and Conrad, O. 2009; Hartemink, A.E. 2015; Mehrnaz, N. *et al.* 2021; Senanayake, I.P. *et al.* 2024).

In addition to spatial surface properties, precision irrigation decision-making traditionally relies on water tension measurements and pF pressure curves, which indicate the pressure required by plants to uptake water under varying moisture conditions (Liang, Z. *et al.* 2020; Lakhiar, I.A. *et al.* 2024). This study, however, introduces a novel approach that incorporates the volume percentage of soil moisture along with the rates of wetting and drying to guide irrigation timing and quantity. While this research does not seek to replace traditional water tension methods, it expands upon them by providing a complementary methodology to improve decision-making for precise agricultural irrigation. Through this, we also aim to highlight the usability of advanced soil monitoring devices, which can be effectively applied within the proposed framework.

Key goals that the current research went for integrating machine learning with spatial interpolation techniques, such as Regression Kriging, to better predict soil moisture variability at smaller scales for water management and complementing pF curves, traditional water tension metrics methodology with time-series soil moisture volume percentages to support controlled irrigation via dynamic state variables calculated from moisture data.

To reach these goals, this study, thus, develops a methodology for the spatial extension of soil water regime variables using geomorphological indicators and high-frequency soil moisture data. This approach aims to create a geographically structured database that can quantify soil water dynamics in the top 20 centimetres across diverse terrain types, including both flat plains and hilly regions. By examining these distinct areas, this study can assess the variability of soil moisture and evaluate its applicability to broader regions. The findings from this research contribute valuable insights into drought and flood-related phenomena, potentially enhancing geographical decision support systems – such as precision agriculture tools – for optimal water resource management.

Materials and methods

The sample areas *(Figure 1)* are presented based on the relevant geographical feature for the research, which is land cover. The diversity of land cover in the areas of interest is significant.

The first sample area, the Cseres Valley, is in the watershed of the Kondó settlement's hilly terrain. The area is characterised by significant geological diversity, with its surface primarily composed of Mediterranean shal-

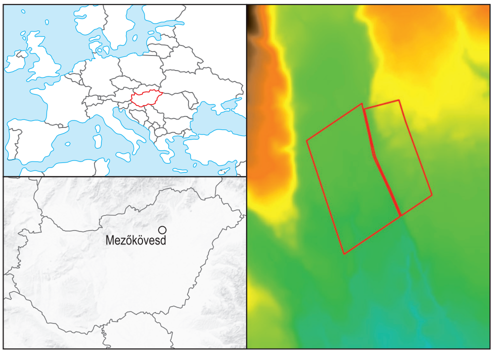

Fig. 1. Location of Mezőkövesd study area

low marine sediments that advanced during the Miocene Badenian and Carpathian epochs (approximately 17 million years ago) (Juhász, A. 1970). The geological landscape of the area exhibits considerable variability over geological epochs. During glaciations, degradation through frost weathering was prevalent, while in interglacial periods, increased precipitation caused linear erosion and weathering to be dominant factors (Pinczés, Z. *et al.* 1993; Harangi, Sz. 2001). Soil movements, both during glacial (cryoturbation, gelifluction) and interglacial periods (gelifluction, solifluction), shaped the surface. Sediment deposition occurred with varying efficiency during the Villányian, Biharian, and Pilisian stages (Dobos, A. 2002). The entire area of the Cseres Valley belongs to the Formation of Egyházasgerge (eMK), with gravel conglomerate found deep down, covered by sand, sandstone, and finer silt and clay on the surface (Gyalog, L. 1996).

The Cseres Valley is V-shaped, 1.6 km long, and 665 m wide, narrowing at the valley throat, with a watershed area of 0.76 km^2. The valley is incised into the terrain to depths of 4–5 metres in places. Several erosional gullies of varying degrees of development, caused by rainfall, accompany the valley, and since 2010, these have also been shaped by the periodic (from spring to autumn) flash floods (Vágó, J. 2012). The area falls within the forest soil zone. The soils identified so far are luvisols, stagnic luvisols, and gleysols. Their common characteristic is high compactness, which is attributed to land use. Most of the valley has been used primarily as pasture or orchards, with smaller forests found on steeper slopes and in the valleys. Cultivated fields and meadows are located on more suitable areas of the slopes, where the signs of machinery work (machine tracks) are evident and are also reflected in the structure of the soils.

Ancient maps suggest that land use has remained unchanged for several centuries. The distribution of soil types from higher elevations to lower ones is as follows: strongly eroded brown forest soil with levissage near the hilltops and watershed ridges, predominantly anthropogenic colluvial soil in the middle of the slope due to its local position, eroded and heavily compacted brown forest soils on the north- and south-facing slopes. At the valley bottom, repeatedly buried gleysoils deposited by cyclical flash floods in the valley, followed by deposited meadow soil rich in anthropogenic materials at the edge of the settlement zone (Dobai, A. and Dobos, E. 2023).

The studied area is moderately warm and moderately dry around 2050. The annual average temperature ranges from 8.8–9.3 °C. The average maximum temperatures on the hottest summer days range from 31–33 °C, while the average minimum temperatures on the coldest winter days are around -17 °C. Annual precipitation ranges from 550–600 mm. The predominant wind directions are NW and SE, corresponding to the terrain, with an average wind speed of 2.5 m/s (Péczely, Gy. 2006; Dövényi, Z. 2010).

In contrast to the previous area, the sample area located near the town of Mezőkövesd on the Bükk pediment exhibits somewhat greater diversity, with stronger manifestations of Luvic Chernozems and gleyic characteristics, previously traversed terraces (see *Figure 1*). The area consists of a mixture of material eroded from the Bükk Mountains and sediment from the Hór Stream. Corresponding to the topography, soil erosion is significant, with the thickness of the humus layer primarily determined by the extent of erosion.

Humus layers ranging from 30 to 80 cm in depth disappear on the slopes, giving way to heavily clayey parent rock. In extreme cases, erosion is halted by the omnipresent calcium carbonate accumulation layer, resulting in patches of calcareous soils.

The area is predominantly characterised by vertisols formed on highly expansive clayey alluvial sediments in the lower parts of the hills, exhibiting good water retention capacity but cracking to depths of 100–130 cm when dry, with cracks 3–7 cm wide. Surface organic matter is sporadically distributed throughout the profile. The filling of cracks leads to loss of free space, and upon rewetting, the expansive clay exerts strong pressure on soil structural elements, resulting in the formation of slickensides, even at depths of 50 cm. These processes result in heavily compacted soils. The high clay content is mitigated in the Hór Valley bottom areas, where loess, loamy material forms the upper 40–80 cm. Chernozem brown forest soils are found only in the southern corners, with the upper layers throughout the profile being formed by loess.

A significant portion of the studied area falls on the bottom of the Hór Valley, where we find alluvial soils mixed with gravel and tuff debris in areas where the Hór Stream previously meandered. In areas where the Hór formed smaller alluvial cones along abandoned channels, loess forms the upper layers of the soil. Strong water influence is not characteristic of the area. Due to the high clay content of Vertisols, signs of stagnant water are present throughout the profile, albeit not pronounced. The alluvial deposits in the valley bottoms, characterised by iron-humic dark colouring and iron and manganese spotting, also indicate water influence, although without a distinct meadow character. Groundwater influence is not observed. The regulated flow of the Hór quickly subsides below the reservoir when water reaches the lower section, with only surface runoff characteristic on the interfluves. Due to the high clay content, infiltration is relatively low. On the sloping hillside surfaces, water drains quickly. Although the process of steppe formation is underway, the soil water regime remains positive (Chernozem brown forest soils), thus, salt accumulation is not expected. Due to the previous loess cover, clays are enriched with basic cations, with calcium being the most characteristic, but magnesium content is also notably high among the basic cations typical of loess. Due to monocultural farming, the flora and fauna of the sample areas are monotonous, with some colour provided by the young, planted forests of the Kondó sample area. Their land use generally consists of abandoned or active arable land.

Monitoring methodology and data processing

The decision-making system starts and works with the entity of our soil monitoring system, the Sentek soil moisture sensors. The Sentek soil moisture sensors operate based on electrostatic interaction, using a capacitive method, where the volumetric water content is derived from the dielectric constants of soil, water, and air, with the unit of measure being volumetric percentage (%). The devices respond even with the smallest changes in moisture content because a relatively low amount of water has a high dielectric constant, significantly increasing the dielectric constant of the mixture of the three elements (water, air, soil) (Al-Ghobari, H.M. and El Marazky, M.S.A. 2013). The electrical capacitance can vary depending on the soil, specifically on the proportions of the three elements and their chemical properties. Therefore, calibration of the sensor is required before measurement, considering the physical properties of the soil, primarily its mechanical composition (Kibirige, D. and Dobos, E. 2021).

The data processing began with the soil moisture data time series collected by the Sentek soil moisture sensors. The purpose was to create a database compiled for each sensor, from which soil water regime variables could be calculated, well reflecting the periodic changes in soil moisture at twenty centimetres depth of the soil. Soil moisture measurements were taken between 2019 and 2022 in the pilot area, with at least one year's worth of temporal data available for each sensor with a two-hour temporal resolution for Mezőkövesd. Since the soil moisture data originates from a depth of 20 cm, evaporation is the most significant climatic factor that can be detected in the soil moisture fluctuations across different seasons *(Figure 2).* Generally, these values are opposite from season to season.

Due to the variability of these values, it is not possible to create new, universally applicable variables from the database created from the measured data. Therefore, examination periods like season combinations were designated to effectively characterize the evaporative conditions of the given period. On Mezőkövesd pilot area (149.74 hectars) two periods – spring-summer and autumn-winter seasons – were chosen. Altogether 13 sensors were available: 6 sensors in the spring-summer season, and 7 ones in the autumn-winter season.

With this period designation, a complex database was created that includes spatial and temporal filtering of the time series data measured in the sample areas, thus, establishing area-specific soil water regime variables. These variables characterize soil properties related to water at the measurement points (Stefanovits, P. 1999; Deák, T. *et al.* 2022), which were the following:

– Infiltration and drying rate (V/V% / time): Both rates are created from the time series of soil moisture measurements, where a new variable was created that contains the value differences between the soil moisture measurements. The new variable contains negative and positive difference values and was further filtered by taking the average value of positive and negative difference values separately. The average calculated from the negative values resulted in the drying rate, while the positive values resulted in the infiltration rate. Only the spring/summer dataset was used for the calculation of these rates as the value changes in the infiltration and drying periods are more present during these seasons and represent these variable conditions (see *Figure 2*).
– Total porosity (V/V%): This value represents the highest measured soil moisture value during the logging, where the thick and thin pores of the layer completely exclude air and get fully saturated with water. The autumn/winter dataset was used for the calculation because the lower temperature and evaporation conditions make the finding easier and more representative.
– Minimal water content (V/V%): This value represents the lowest measured soil mois-

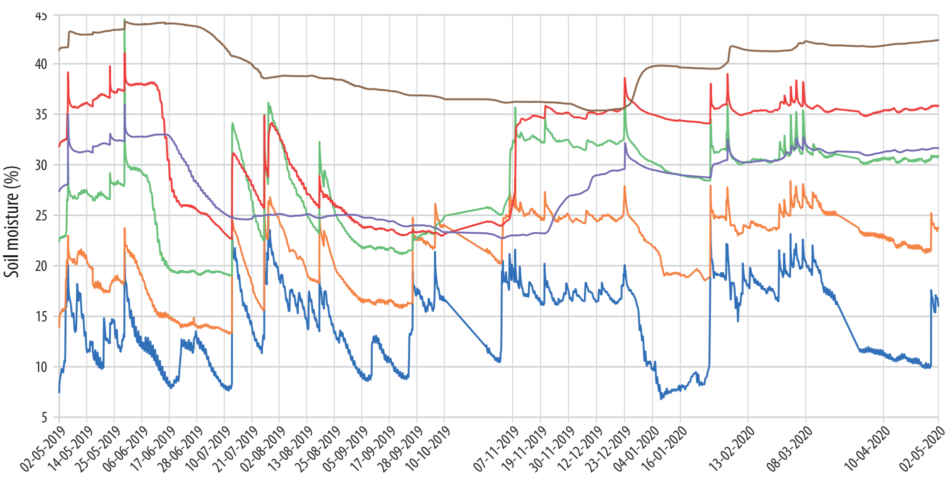

Fig. 2. Changes of soil moisture between 02.05.2019 and 02.05.2020 in Mezőkövesd. *Source*: Authors' compilation.

ture value during the logging. The spring/summer dataset was used because of the higher temperature and evaporation conditions in Hungary (Péczely, Gy. 2006; Dövényi, Z. 2010).

– Water holding capacity range (V/V%): This value was calculated by subtracting the minimal water content from the total porosity, which shows the range within which the soil moisture can change. In this case, the whole yearly time series dataset was used since none of the seasonal conditions affect this variable, and the most amount of data is needed to find the widest range of change in terms of soil moisture.

Since only point-wise target variables measured by the sensors within the sample areas are available, spatially independent auxiliary variables had to be employed to aid the extension and reduce statistical uncertainty (Bock, M. *et al.* 2007). Thus, 14 independent geomorphological variables (GVs) were defined created from digital elevation models of each sample area with a spatial resolution of 5 metres *(Table 1).*

The GVs created from the "Basic Terrain Analysis" module of a desktop-based geographic information system (GIS) were called SAGA-GIS (Conrad, O. *et al.* 2015). The spatial extension was performed using Regression Kriging, which is a methodology that utilizes spatial estimation, combining spatial correlation from Kriging with the pixel value estimation from many choosable regression models (Hengl, T. *et al.* 2007). In this case, for Kriging, the Ordinary Kriging and for a regression model, Random Forest (RF) were employed as the default methods, commonly used for spatial extension of environmental variables in geostatistics (Hengl, T. *et al.* 2018).

Table 1. List of available geomorphological variables (GVs)

Closed Depression	Profile Curvature
Convergence Index	Plan Curvature
Closed Depression	Relative Slope Position
Channel Network Base Level	Slope
Channel Network Distance	Total Catchment Area
Relative Relief	Topographical Wetness Index
LS-Factor	Valley Depth

The study involved analyzing sample areas with different geomorphological characteristics. Consequently, different GVs were always crucial for the spatial extension of a given variable. To determine this, only specific variables can be used due to the collinearity of the variables. Picking GVs required a set of rules, which were the following:

– The amount of GVs can't be more than the number of points (training data) used for the spatial extension due to the curse of dimensionality (Ying, X. 2019).

– The GVs need to have the lowest correlation between them hence the independence of these variables.

After setting these rules, a Pearson correlation analysis (Sedgwick, P. 2012) was used to determine a list of independent variables which will be used for the spatial extension of the water regime variables *(Figure 3).* The steps were the following:

1. The first independent GV was chosen based on how many other GVs had a correlation between 0.03 and -0.03. The one with the most variables that would fit this rule would be the first while the remainers were the ones that picked by the correlation threshold (0.03) inside what was available for the first GV.

2. In this case, the "Slope" GV had 4 variables, the greatest number of variables within the correlation threshold. The "Slope" variable was the first, while the remainers were the Convergence Index, Plan Curvature, Profile Curvature and the Relative Relief (see *Figure 3*). These remainers were inside the correlation threshold compared to the first, picked "Slope" GV.

3. If there are two or more cases where every variable had the number of variables, then it would be decided which had the lowest average correlation value. This was not the case in our correlation analysis, but this rule was brought up for replication.

The picked GVs are used in basic terrain analysis like slope and curvature types of the terrain with some more complex ones like the conver-

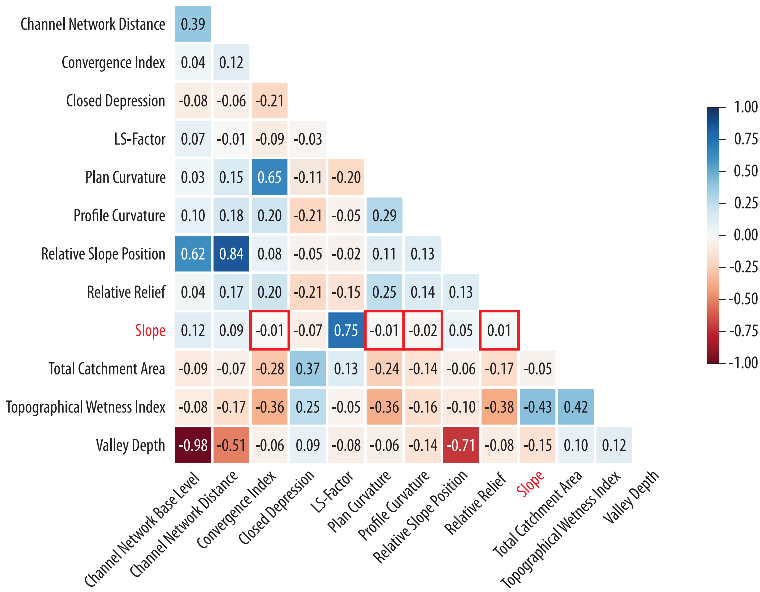

Fig. 3. Correlation matrix between the GVs derived from the DEM representing the Mezőkövesd pilot area and the picked independent variables highlighted with red borders and text. *Source*: Authors' compilation.

gence index, which shows the extent of either convergence or divergence by pixel (Kiss, R. 2004) and the relative relief, which was calculated by dividing the pixel values of the focal average from the digital elevation model.

Validation of the infiltration rate variable using on field infiltration measurements

During the data collection of soil moisture values via the Sentek sensors, on field infiltration experiments were done on Kondó, in the same sensor positions during the summer of 2022. These experiments aim to measure the infiltration rate with field tools so it can be used for validation and comparison to the infiltration rate variable made from the time series soil moisture readings.

This experiment extended to three Sentek positions *(Figure 4)* on field with constant head infiltration measurements. The main purpose of the method used is to measure the amount of water infiltrating into the soil per unit of time by placing two metal frames on the soil. The outer frame provides constant hydrostatic pressure to ensure that the water in the inner frame infiltrates deeper into the soil and does not escape laterally (Várallyay, Gy. and Fórizs, J. 1966).The measuring process involved fully saturating the area around the Sentek sensors with water and then gradually measuring how much water infiltrated over time for at least 2 hours. These measurements were then converted to the same temporal resolution as that of the Sentek sensors, resulting in one predicted soil moisture measurement in V/V% per two hours.

Implementing Leave-One-Out Cross-Validation for the spatial extension of water regime variables for validation

The model performance evaluation cannot be done by splitting the data due to the already low amount of points usable for spatial extension.

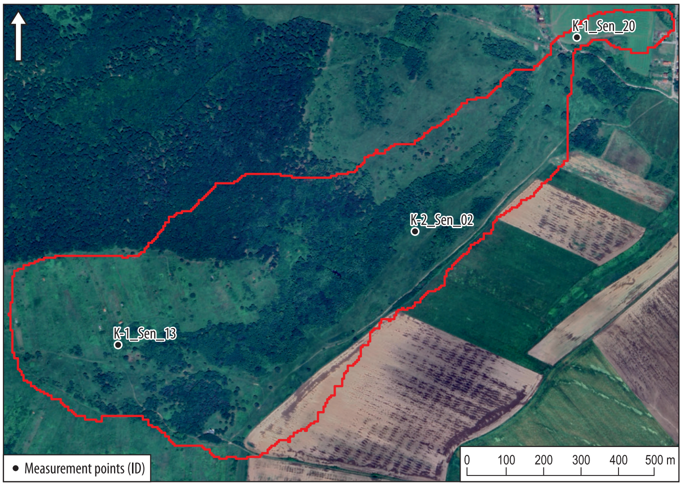

Fig. 4. Pilot area of Kondó featuring the sensor/field measurement points. *Source*: Authors' compilation.

A different validation methodology was needed, and Leave-One-Out Cross-Validation (LOOCV) was chosen for this reason (Berrar, D. 2019). This validation process requires the creation of several models and values from an evaluation metric of choice. The model creation happens by making as many iterations as many points are available. At each iteration, we create a model with one less point. This point is the test data, while the remainer points are the training data for that model iteration. Every iteration shows a different point taken out as a test point.

In this case, each water regime variable had six iterations *(Figure 5)* (except for total porosity with seven used from the autumn/winter dataset – *Figure 6*) of models with their own evaluation metric which was root mean square error (RMSE) in our case.

Results and discussion

Monitoring

While the spatial extension of each water regime variable used the same list of independent variables, depending on the iteration, the results were different.

Infiltration and drying rate

Both rate variables have their lowest RMSE values on the fourth iteration *(Table 2).* In terms of spatial extension, they are correlating with each other regarding how values are distributed around the pilot area. The best areas when it comes to drying and infiltration are located on the north-western side of the plot area, while the worst on the southern half with distinguishable, natural topographic features such as the side valley of the Hór stream bearing the lowest drying and infiltration values *(Figure 7).*

Due to the veiny, thinner look and spatial distribution of the pilot area, the convergence index could be the most related when predicting drying and infiltration rates for the area (see *Figure 7*).

Total porosity

For total porosity, it was the only variable with one more iteration plus compared to the others, resulting in the fourth iteration as the worst, which was the complete opposite of the rate variables (see *Table 2*). However, it only took one more iteration to be the best, resulting the

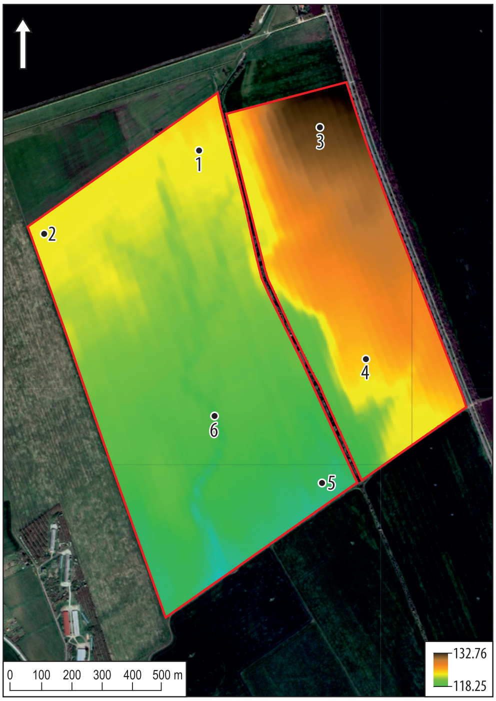

Fig. 5. Iteration order of the left out points (test data) for the spatial extension of all water regime variables (except total porosity). *Source*: Authors' compilation.

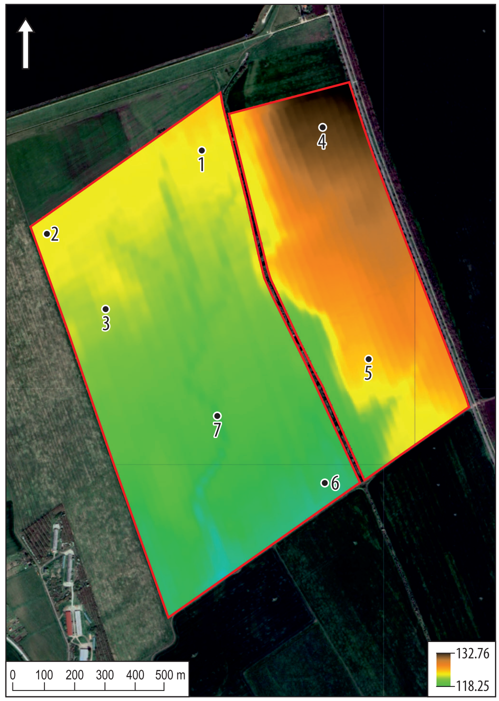

Fig. 6. Iteration order of the left out points (test data) for the spatial extension of total porosity. *Source:* Authors' compilation.

Table 2. RMSE values of each model iteration for every water regime variable

Iterations	Infiltration rate	Drying rate	Total porosity	Minimum water content	Water holding capacity
	V/V% / 2 hour		V/V%		
1	0.041799	0.022277	0.670538	4.074932	0.179433
2	0.044332	0.020514	0.855228	3.736326	0.013592
3	0.024276	0.016299	0.017738	3.620505	1.071288
4	0.000161	0.000605	1.582832	3.495494	0.011158
5	0.036959	0.017024	0.006760	2.856400	0.009271
6	0.030051	0.018315	0.007070	0.012209	0.006486
7	–	–	0.013099	–	–

lowest RMSE value in the fifth iteration. When it comes to the spatial distribution, there is a northern and southern split in terms of values.

However, the split is not as homogeneous. There is also a split between the artificially created valleys defined by the north-western sowing direction of the plot area (see *Figure 6*). By checking GVs that greatly distinguish micro valleys like the DEM and convergence index, it's obvious how the sowing direction changed the micro topology of the area while also highlighting holes in between them referring to the natural topological features like side stream valleys (see *Figure 7*).

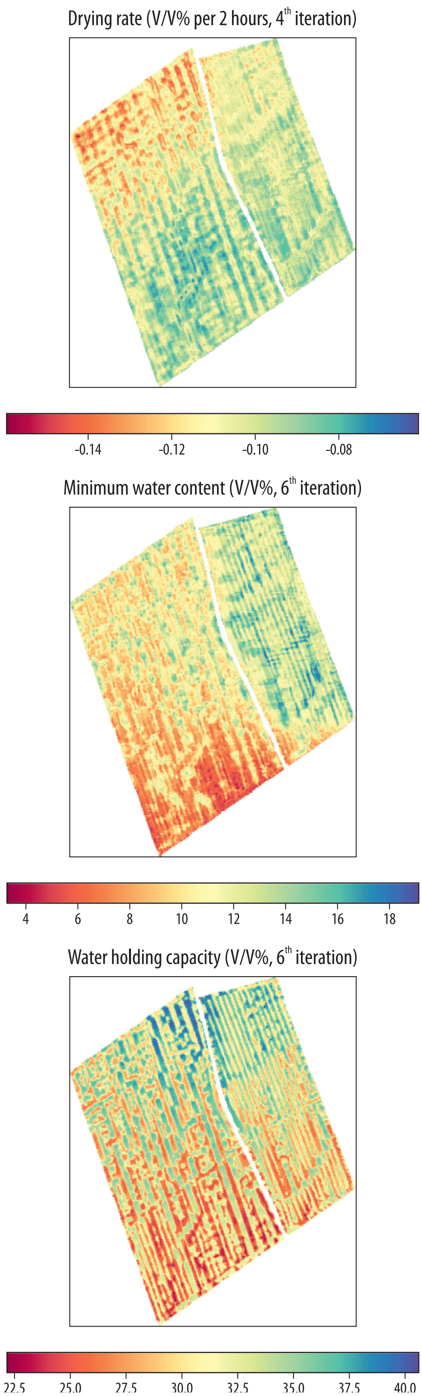

Fig. 7. Each water regime variable's best iteration of spatial extension in terms of RMSE value from the Mezőkövesd pilot area. *Source*: Authors' compilation.

Higher values can be found in lower micro valleys, where material convergence is intact, while lower values are on micro ridges throughout the whole plot area. Due to the presence of natural side valleys, these artificial valleys and ridges are not constant but separated in areas where a direction change happens along the surface. These areas are well represented by the slope and curvature GV's (see *Figure 7*).

Minimal water capacity

For minimal water capacity, the sixth iteration was the best regarding RMSE value (see *Table 2*). The spatial distribution is most homogenous compared to the other water regime variables, where there is an east and west value split (see *Figure 7*).

Highlighted lower and higher areas also can be spotted similarly to the total porosity which are side stream valleys. The value split might indicate significance to the elevation of the area, even though DEM was never used as an independent variable for the spatial extension.

However, the relative relief could be the most significant variable in this case as it only generalises the elevation and gives a buffer to the natural side alleys of the area, hence giving a rough look and distribution to those areas where the lowest and highest values are *(Figure 8).*

Water holding capacity range

Water holding capacity range uses the same sixth iteration as its best iteration (see *Table 2*) while also having an almost identical spatial distribution compared to total porosity.

The only real difference is in the artificial micro valleys with lower valued pixels, meaning there is a more significant value difference between artificial topographic features when it comes to the water holding capacity of the pilot area *(Figure 6).*

Validation

In our comparison, we had three sensors of data representing the 2022 spring/summer season, with all of them having in field infiltration measurements. While there were not a lot of sensors around the area which we could use, the results show that the differences can vary between 0 to 46 percent value difference when comparing the infiltration rate calculated from the time series data to the on-field measurements *(Table 3).*

This can be due to the different geomorphological circumstances or the methodology used to calculate each point of infiltration using the drying periods of the time series soil moisture measurements.

Discussion

The methodologies and results in this study contribute to advancing precision irrigation through three key perspectives: methodological, device, and spatial resolution. These enhancements aim to support data-driven irrigation decision-making in agricultural settings with improved accuracy and scalability.

Methodological perspective

One of the foundational principles of digital soil mapping is extending sampled soil properties using spatial interpolation methods, commonly relying on distance-based approaches such as Kriging (Lagacherie, P. *et al.* 2006). However, these methods often struggle when the microtopography highly influences the target variable (e.g., soil moisture) and re-

Table 3. RMSE values of each model iteration for every water regime variable

ID	Field measured	Sensor measured	Difference, %
	V/V% / 2 hour		
K-2_Sen_02	0.11	0.31	20
K-1_Sen_20	0.05	0.51	46
K-1_Sen_13	0.24	0.24	0

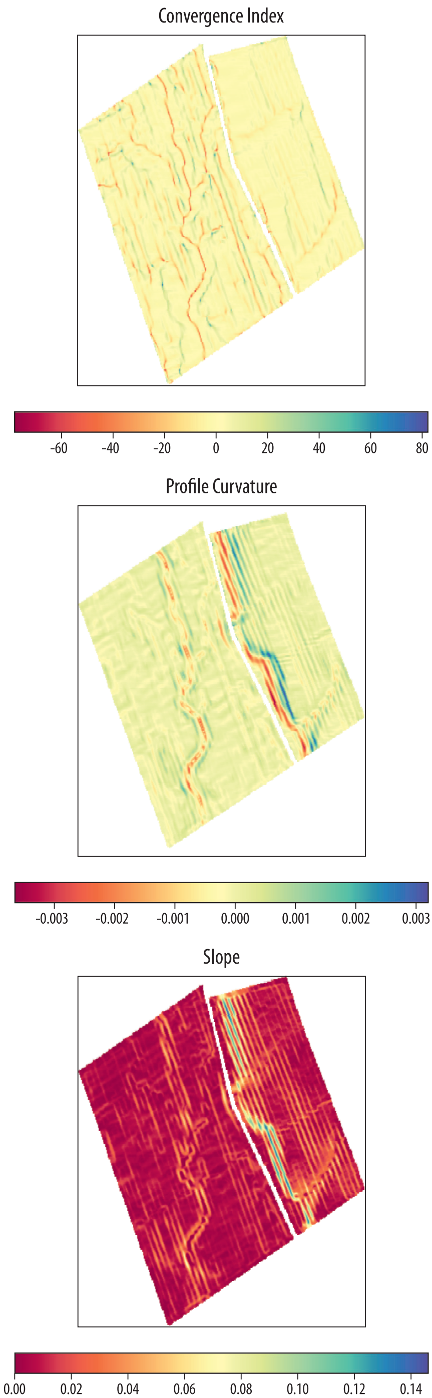

Fig. 8. All independent variables used for the spatial extension of the water regime variables from the Mezőkövesd pilot area. *Source*: Authors' compilation.

quires a high sampling density to capture local variations accurately. For soil moisture, which correlates closely with topographic features (Guo, X. *et al.* 2020; Winzeler, H.E. *et al.* 2022), a pure, distance-based, spatial interpolation approach may produce limited accuracy due to its inability to capture the nuances introduced by geomorphological complexity. This study employed a machine learning approach combined with multiple geomorphological descriptors derived from a 5-metre high-resolution digital elevation model (DEM). By integrating terrain variables with soil moisture data, we created spatially extended variables that reflect not only spatial proximity but also distance in value, accounting for the influence of topographic variability, which is the whole point of using Regression Kriging for spatial extensions (Hengl, T. *et al.* 2007). This hybrid approach enables a more nuanced spatial dataset that captures both spatial transitions and topographic-driven variations in soil moisture and water management variables.

Comparable studies have demonstrated similar benefits of integrating terrain models for soil property mapping (Li, X. *et al.* 2020; Adeniyi, O.D. *et al.* 2024). Still, such methods have been limited mainly to soil physical and chemical attributes while relying on Regression Kriging. Our approach, thus, represents an adaptation of these techniques to soil moisture, extending their applicability to soil water regime variables within high-resolution, localised with agricultural contexts.

Device perspective

Precision irrigation has increasingly adopted tools and methods that align with plant-specific water requirements, with tensiometers being among the most widely used devices to measure soil moisture in response to plants' water needs. Although effective, reliance on tensiometers or similar tension-based devices constrains soil moisture monitoring systems that support precision irrigation (Owino, L. and Söffker, D. 2022). Many existing systems made for these tensiometers are incompatible, creating a gap in expanding irrigation support capabilities using a broader range of affordable, other than the tensiometer, volume-based soil moisture sensors (Abdelmoneim, A.A. *et al.* 2023). The issue isn't that other devices can't be used; rather, compared to water tension methods, there are currently too few effective and scalable alternative methodologies that provide spatial data-based support for precision irrigation without relying on tension meter devices. Our study overcomes this limitation by demonstrating that time-series soil moisture data measured in volume percentage (e.g., using Sentek EnviroSCAN dielectric sensors) can provide comparable insights into soil water regimes.

The methodology developed here enables measurements from dielectric constant-based devices, regardless of depth or logging frequency, to be seamlessly integrated into irrigation support systems. This flexibility significantly broadens the range of feasible soil monitoring setups, from cost-effective 10 cm depth sensors to high-frequency logging, multi-depth, industrial-grade sensors. The adaptability provided here to scale measurements across device types presents an economically viable solution for stakeholders aiming to implement or expand soil monitoring systems within precision irrigation management.

Spatial resolution perspective

Many research, commercial, and governmental entities currently rely on freely available optical remote sensing data for monitoring soil moisture on a broad scale (Joshi, N. *et al.* 2016). While this data is useful for national and regional assessments, its spatial resolution is typically inadequate for precision irrigation at the farm or field level (Dobos, E. *et al.* 2013). Moreover, freely available optical, remote sensing data is generally disconnected from localised topographic influences, which are critical for effective moisture management in undulating or heterogeneous landscapes (Wang, S. *et al.* 2018). Our research addressed this limitation by using high-resolution DEM generated from RTK GPS-measured point clouds with a spatial resolution of 5 metres. From this DEM, we derived GVs – such as elevation, slope, curvature, and other terrain variables – that are essential in characterizing and predicting soil moisture variability at the sub-field level. This resolution enables us to capture and quantify subtle relief factors that influence soil moisture dynamics, providing a more accurate basis for precision irrigation planning. By linking these topographic variables to in situ soil moisture and water management measurements, we created a spatially refined dataset that supports precision agriculture by connecting soil moisture information to local field terrain conditions.

Conclusions

The micro-topographic properties are appropriately reflected in the resulting maps. The elevation model shows that a higher sloped region and former streambeds fundamentally characterize the area. Accordingly, the texture of the soils in the area is varied. On the higher terrain, the soils are clayier, while in the lower areas, they consist of thin sand, sandy loam, and gravelly material from the former streambed. These properties can be quantified by the various geomorphological variables (GV), and these surface characteristics are highlighted. The total porosity map confirms the previously mentioned features and these observations can be further analysed and evaluated on the infiltration, drying, and minimum water content maps. Excluding the water holding capacity dataset results, which may differ in this case, considerations must also be given to field sampling experiences and variability arising from previous datasets.

The relationship between hydrological datasets and GVs entails uncovering the most characteristic and extreme micro-topographic areas within the pilot area first due to factors such as the sensor installation location and the land use. Data collection must be performed on these points (whether for soil sampling or deploying smart devices such as Sentek soil moisture sensors), which can be more challenging in monocultural agricultural fields, where artificial microtopographic features must be considered.

Further improvement in estimation accuracy can be achieved by collecting data at intermediate points within known topographic features, not just at the most extreme endpoints. For example, if it's found during field research that directional changes or other geomorphological features (such as terraces) are present along uniform slopes, it's worthwhile to collect data not only at the lowest and highest points of the slope but also from the in between topographic elements.

The importance of placing these sensors can also be backed up with the iteration order of the spatial extension. Either the first or the second was the worst iteration for almost every water regime variable (see *Table 2*). In real life, these iterations belonged to points which were placed on heights which were in between the lowest and highest heights (see *Figure 7*). This indicates that there is a risk of error if the points are not placed evenly on geomorphological features, be it either natural or artificial (Chen, Y. *et al.* 2021).

The preliminary validation results show that more on field measurements are required at sensor points to have a better understanding of how robust the methodology when creating the infiltration and drying rates just based on time series soil moisture measurements done by the Sentek sensors. Validation of the other water regime variables is also a future goal for this ongoing research, which can be expanded by collecting soil samples and comparing soil physical parameters that can be used and correlated to validate these variables.

Looking at the list of independent variables, the picked variables correlate to the artificial topographic features located in an agriculturally heavily used area. Slope and curvature types clearly represent the constant direction changes of the landscape. While the 5-metre spatial resolution was not enough to clearly spot it, new, significant, artificially created micro valleys are being developed over time, which can be detected in the convergence index (see *Figure 8*). These micro valleys also contribute to the poor water circulation which clearly shows the predicted water capacity range and total porosity maps (see *Figure 7*). This is due to the constant, intensive agriculture.

Overall it can be concluded that the methodology can provide a suitable foundation for the initial determination of soil water regime characteristics, thereby aiding in precision agriculture and irrigation development. Future research directions will aim to incorporate additional sample areas, densify field training and test points, and further strengthen the current results.

***Acknowledgement*:** The research was carried out with funding by the 2020-1.1.2-PIACI-KFI: Support for Market-Driven Research, Development, and Innovation Projects – Development of an ICT Platform for Supporting Soil Information-Driven Agriculture for Managing and Optimizing Agricultural Production and Monitoring the Effects on the Soil System, and funding by the RRF-2.3.1-21-2022-00014 Climate Change Multidisciplinary National Laboratory for Climate Change.

REFERENCES

Abdelmoneim, A.A., Khadra, R., Elkamouh, A., Derardja, B. and Dragonetti, G. 2023. Towards affordable precision irrigation: An experimental comparison of weather-based and soil water potential-based irrigation using low-cost IoT-tensiometers on drip irrigated lettuce. *Sustainability* 16. (1): 306. https://doi.org/10.3390/su16010306

Adeniyi, O.D., Bature, H. and Mearker, M. 2024. A systematic review on digital soil mapping approaches in lowland areas. *Land* 13. (3): 379. https://doi.org/10.3390/land13030379

Al-Ghobari, H.M. and El Marazky, M.S.A. 2013. Field evaluation of EnviroSCAN performance for monitoring soil water content compared with other soil moisture sensors under arid conditions. *Wulfenia Journal* 20. (4): 54–70.

Berrar, D. 2019. Cross-validation. In *Reference Module in Life Sciences. Encyclopedia of Bioinformatics and Computational Biology.* Vol. 1. Eds.: Ranganathan, S., Gribskov, M., Nakai, K. and Christian Schönbach, C., Amsterdam, Elsevier, 542–545. https://doi.org/10.1016/B978-0-12-809633-8.20349-X

Bock, M., Böhner, J., Conrad, O., Köthe, R. and Ringeler, A. 2007. *XV. Methods for Creating Functional Soil Databases and Applying Digital Soil Mapping with SAGA GIS*. JRC scientific and technical reports. Luxemburg, Office for Official Publications for the European Communities.

Chen, Y., Hou, J., Huang, C., Zhang, Y. and Li, X. 2021. Mapping maize area in heterogeneous agricultural landscape with multi-temporal Sentinel-1 and Sentinel-2 images based on random forest. *Remote Sensing* 13. (15): 2988. https://doi.org/10.3390/rs13152988

Conrad, O., Bechtel, B., Bock, M., Dieztrich, H., Fischer, E., Gerlitz, L., Wehberg, J., Wichmann, V. and Böhner, J. 2015. System for Automated Geoscientific Analyses (SAGA) v. 2.1.4. *Geoscientific Model Development* 8. 1991–2007. https://doi.org/10.5194/gmd-8-1991-2015

Deák, T., Dobos, E. and Kovács, Z.K. 2022. Talajnedvesség beszivárgási intenzitás számítása high-tech szenzorok segítségével (Calculation of soil moisture infiltration intensity with the help of high-tech sensors). In *Tavaszi Szél 2022*. Tanulmánykötet I. Eds.: Molnár, Dá., Molnár, Dó. and Nagy, A.Sz. Budapest, Doktoranduszok Országos Szövetsége (DOSZ), 238–255.

Dobai, A. and Dobos, E. 2023. Beszivárgás vizsgálat a Cseres-völgyben (Infiltration study in the Cseres Valley). *Talajvédelem 2023.* Különszám. 40–55.

Dobos, A. 2002. A Bükkalja II. Felszínalaktani leírás (Surface morphological description of Bükkalja II). In *A Bükki Nemzeti Park*. Ed.: Baráz, Cs. Eger, Bükki Nemzeti Park Igazgatóság, 217–227.

Dobos, E., Michéli, E., Baumgardner, M.F., Biehl, L. and Helt, T. 2000. Use combined digital elevation modell and satellite radiometric data for regional soil mapping. *Geoderma* 97. 367–391. https://doi.org/10.1016/S0016-7061(00)00046-X

Dobos, E. and Daroussin, J. 2005. The derivation of the potential drainage density index (PDD). In *An SRTM-Based Procedure to Delineate SOTER Terrain Units on 1:1 and 1:5 millions scales.* By Dobos, E., Daroussin, J. and Montanarella, L., Luxemburg, Office for Official Publications for the European Communities, Luxemburg, 40–45.

Dobos, E., Seres, A., Vadnai, P., Michéli, E., Fuchs, M., Láng, V., Bertóti, R.D. and Kovács, K. 2013. Soil parent material delineation using MODIS and SRTM data. *Hungarian Geographical Bulletin* 62. (2): 133–156. Available at https://ojs3.mtak.hu/index.php/hungeobull/article/view/2951

Dövényi, Z. (ed.) 2010. *Magyarország kistájainak katasztere* (Inventory of microregions in Hungary). Budapest, MTA Földrajztudományi Kutató Intézet.

Garcia, L.D., Lozoya, C., Favela-Contreras, A. and Giorgi, E. 2023. A comparative analysis between heuristic and data-driven water management control for precision agriculture irrigation. *Sustainability* 15. (14): 11337. https://doi.org/10.3390/su151411337

Guo, X., Fu, Q., Hang, Y., Lu, H., Gao, F. and Si, J. 2020. Spatial variability of soil moisture in relation to land use types and topographic features on hillslopes in the black soil (mollisols) area of northeast China. *Sustainability* 12. (9): 3552. https://doi.org/10.3390/su12093552

Gyalog, L. 1996. *A földtani térképek jelkulcsa és a rétegtani egységek rövid leírása* (Legend of geological maps and brief description of stratigraphic units). Magyar Állami Földtani Intézet Alkalmi Kiadványa 187. Budapest, MÁFI.

Harangi, Sz. 2001. Neogene to Quaternary volcanism of the Carpathian-Pannonian Region – A review. *Acta Geologica Hungarica* 44. (2–3): 223–258.

Hartemink, A.E. 2015. The use of soil classification in journal papers between 1975 and 2014. *Geoderma Regional* 5. 127–139. https://doi.org/10.1016/j.geodrs.2015.05.002

Hengl, T., Heuvelink, G.B. and Rossiter, D.G. 2007. About Regression-Kriging: From equations to case studies. *Computers & Geosciences* 33. (10): 1301–1315. https://doi.org/10.7717/peerj.5518

Hengl, T., Nussbaum, M., Wright, M.N., Heuvelink, G.B. and Gräler, B. 2018. Random forest as a generic frame work for predictive modeling of spatial and spatio-temporal variables. *PeerJ* 6. e5518. https://doi.org/10.3390/rs8010070

Joshi, N., Baumann, M., Ehammer, A., Fensholt, R., Grogan, K., Hostert, P., Jepsen, M.R., Kuemmerle, T., Meyfroidt, P., Mitchard, E.T.A., Reiche, N., Ryan, C.M. and Waske, B. 2016. A review of the application of optical and radar remote sensing data fusion to land use mapping and monitoring. *Remote Sensing* 8. (1): 70. https://doi.org/10.3390/rs8010070

Juhász, A. 1970. A Borsodi-medence keleti részén a helvéti barnakőszéntelepek szénkőzettani, településtani vizsgálata (Coal geology and settlement studies of the helvetic brown coal deposits in the eastern part of the Borsod Basin). *Földtani Közlöny* 100. 239–306.

Kibirige, D. and Dobos, E. 2021. Off-site calibration approach of EnviroScan capacitance probe to assist operational field applications. *Water* 13. (6): 837. https://doi.org/10.3390/w13060837

Kiss, R. 2004. Determination of drainage network in digital elevation models, utilities and limitations. *Journal of Hungarian Geomathematics* 2. 17–29. Available at https://real.mtak.hu/121965/1/Kiss_Richard_JHG.pdf

Laborczi, A., Bozán, C., Körösparti, J., Szatmári, G., Kajári, B., Túri, N., Kerezsi, Gy. and Pásztor, L. 2020. Application of hybrid prediction methods in spatial assessment of inland excess water hazard. *ISPRS International Journal of Geo-Information* 9. (4): 268. https://doi.org/10.3390/ijgi9040268

Lagacherie, P., McBratney, A. and Voltz, M. 2006. *Digital Soil Mapping – An Introductory Perspective.* Amsterdam, Elsevier.

Lakhiar, I.A., Yan, H., Zhang, C., Wang, G., He, B., Hao, B., Han, Y., Wang, B., Bao, R., Syed, N.T., Chauhdary, J.N. and Rakibuzzaman, Md. 2024. A review of precision irrigation water-saving technology under changing climate for enhancing water use efficiency, crop yield, and environmental footprints. *Agriculture* 14. (7): 1141. https://doi.org/10.3390/agriculture14071141

Li, X., McCarty, G.W., Du, L. and Lee, S. 2020. Use of topographic models for mapping soil properties and processes. *Soil Systems* 4. (2): 32. https://doi.org/10.3390/soilsystems4020032

Liang, Z., Liu, X., Xion, J. and Xiao, J. 2020. Water allocation and integrative management of precision irrigation: A systematic review. *Water* 12. (11): 3135. https://doi.org/10.3390/w12113135

Mehrnaz, N., Fereydoon, S., Azam, J., Ali, K. and Amin, S. 2021. Digital mapping of soil classes using spatial extrapolation with imbalanced data. *Geoderma Regional* 26. 2021. https://doi.org/10.1016/j.geodrs.2021.e00422

Olaya, V. and Conrad, O. 2009. Geomorphometry in SAGA. *Developments in Soil Science* 33. 293–308. https://doi.org/10.1016/S0166-2481(08)00012-3

Owino, L. and Söffker, D. 2022. How much is enough in watering plants? State-of-the-art in irrigation control: Advances, challenges, and opportunities with respect to precision irrigation. *Frontiers in Control Engineering* 3. 982463. https://doi.org/10.3389/fcteg.2022.982463

Péczely, Gy. 2006. Magyarország éghajlata (Climate of Hungary). In Éghajlattan. By Péczely, Gy., Budapest, Nemzeti Tankönyvkiadó, 258–284.

Pinczés, Z., Martonné Erdős, K. and Dobos, A. 1993. Eltérések és hasonlóságok a hegylábfelszínek pleisztocén felszínfejlődésében (Differences and similarities in the Pleistocene surface evolution of foothill areas). *Földrajzi Közlemények* 117. (3): 149–162.

Sedgwick, P. 2012. Pearson's correlation coefficient. *BMJ* 345. e4483. https://doi.org/10.1136/bmj.e4483

Senanayake, I.P., Hancock, G.R. and Welivitiya, W.D.D.P. 2024. Soil depth and catchment geomorphology: A field, vegetation and GIS based assessment. *Geoderma Regional* e00824. https://doi.org/10.1016/j.geodrs.2024.e00824

Stefanovits, P. 1999. *Talajtan* (Pedology). Budapest, Mezőgazda Kiadó.

Vágó, J. 2012. *A kőzetminőség szerepe a Bükkalja völgy- és vízhálózatának kialakulásában* (The role of rock quality in the formation of the Bükkalja valley and hydrological network). Doctoral thesis, Miskolc, University of Miskolc.

Van de Broek, M., Henriksen, C.B., Ghaley, B.B., Lugato, E., Kuzmanovski, V., Trajanov, A., Debeljak, M., Sandén, T., Spiegel, H., Decock, Ch., Creamer, R. and Six, J. 2019. Assessing the climate regulation potential of agricultural soils using a decision support tool adapted to stakeholders' needs and possibilities. *Frontiers in Environmental Science* 7. 131. https://doi.org/10.3389/fenvs.2019.00131

Várallyay, Gy. and Fórizs, J. 1966. A helyszíni talajfelvételezés módszertana (Methodology of in situ soil survey). *In A genetikus üzemi talajtérképezés módszerkönyve.* Ed.: Szabolcs, I., Budapest, Táncsics Könyvkiadó, 19–164.

Wang, S., Lu, X., Cheng, X., Li, X., Peichl, M. and Mammarella, I. 2018. Limitations and challenges of MODIS-derived phenological metrics across different landscapes in Pan-Arctic regions. *Remote Sensing* 10. (11): 1784. https://doi.org/10.3390/su16010306

Winzeler, H.E., Owens, P.R., Read, Q.D., Libohova, Z., Ashworth, A. and Sauer, T. 2022. Topographic wetness index as a proxy for soil moisture in a hillslope catena: Flow algorithms and map generalization. *Land* 11. (11): 2018. https://doi.org/10.3390/land11112018

Ying, X. 2019. An overview of overfitting and its solutions. *Journal of Physics:Conference series* 1168. (2): 022022. https://doi.org/10.1088/1742-6596/1168/2/022022